FireFinder: A Feature-Centric Pipeline for Robust Fire Detection in Images

Ladan Tazik[1], Jacob Tizel[1], Beck Corkle[1], Zoe Dale[1], Seth Richard[2]
[1]*Department of Computer Science, University of British Columbia, Okanagan Campus*
[2]*School of Engineering, University of British Columbia, Okanagan Campus*

Abstract

Accurate and timely fire detection is critical for minimizing damage and improving response in hazardous environments. This study presents a pixel-wise fire detection pipeline that combines color and texture features to improve classification performance. We extract color information from multiple color spaces and apply Gabor filters to capture spatial texture patterns associated with fire. The resulting compact feature set is evaluated using both logistic regression and LightGBM classifiers. Our approach outperforms models trained on individual color spaces across all key metrics, achieving up to 90.68% accuracy with LightGBM and demonstrating significant improvements in precision, recall, and false positive rate. These results highlight the benefit of integrating complementary spectral and spatial features for robust fire detection. The effectiveness of the system, even with simple models, suggests a strong potential for deployment in real-time and resource-constrained settings.

1 Introduction

Computer vision, a subfield of artificial intelligence, enables machines to interpret and analyze visual data, playing a crucial role in applications such as medical imaging, autonomous vehicles, surveillance, and disaster response. One critical application is fire detection, particularly in the context of early wildfire warning systems. As the frequency and intensity of wildfires increase due to climate change, there is a growing demand for fast, reliable, and cost-effective fire detection methods.

Fire monitoring systems typically fall into three categories: ground-based sensors, satellite-based imaging, and unmanned aerial vehicles (UAVs). Although ground sensors can continuously monitor fire-prone areas, they suffer from limited spatial coverage and are prone to human error. Satellites provide broad-area observations but at low temporal resolution, often detecting fires only after significant growth. UAVs, on the other hand, offer a practical balance with high-resolution real-time image acquisition over wide and remote areas (Ghali et al., 2020).

In this context, vision-based fire detection methods have emerged as promising tools to analyze still images and video feeds. These methods generally rely on visual features, primarily color, shape, texture, and motion, to distinguish fire from non-fire regions. However, several challenges remain. Fire often appears in various forms depending on environmental conditions, and non-fire objects (e.g., sunlit surfaces and reflections) may exhibit fire-like colors. In addition, factors such as variable illumination, haze, and complex backgrounds introduce noise that can lead to false positives and missed detections (Toulouse et al., 2017; Umamaheshwaran et al., 2006; Zarkasi et al., 2019).

Color-based segmentation has long been a foundational technique in fire detection due to the strong chromatic signatures of flames, especially in the red-yellow range. Thresholding methods applied in RGB, HSV, or YCbCr spaces are computationally efficient, but often suffer from poor generalization under varied lighting. To improve robustness, researchers have explored hybrid approaches that integrate both spectral and spatial information. Texture features, in particular, can provide valuable cues about the irregular and flickering nature of fire. Among available descriptors, Gabor filters are well-suited for capturing local frequency and orientation patterns typical of flames. When used alongside color segmentation, Gabor filtering can help distinguish true fire regions from visually similar background artifacts.

In this study, we present a comparative analysis of

four commonly used color spaces, RGB, HSV, YCbCr and L*a*b each combined with Gabor texture filtering to identify fire pixels in still images. The objective is to evaluate how the integration of spatial texture features with chromatic information impacts fire detection accuracy. Ground truth fire masks are used to quantitatively assess each hybrid model's performance, and generalization is evaluated using unseen data. This work contributes to the growing body of research on interpretable traditional computer vision techniques for fire detection and underscores the potential of hybrid models to improve detection reliability without the computational burden of deep learning.

2 Related Works

Fire detection in still images has been widely explored using classical computer vision techniques. Deep learning approaches, particularly those utilizing Convolutional Neural Networks (CNNs), demonstrate superior accuracy and robustness (Xiong, 2020; Ajay Bhosle, 2024) but require extensive annotated datasets, high computational resources, and tend to lack interpretability. Unlike deep learning methods, classical computer vision techniques do not require large labeled datasets or expensive hardware, making them more suitable for real-time applications in constrained environments. While effective in specific contexts, these approaches often suffer in the presence of noise factors such as illumination changes, reflective surfaces, and atmospheric distortions. To overcome these limitations, recent studies have emphasized the importance of hybrid systems that combine complementary cues—such as motion and texture—to improve detection robustness.

Color segmentation remains a foundational method for fire detection, particularly in RGB, HSV, and YCbCr spaces. Threshold-based rules targeting high red intensity, low chrominance, or specific hue-saturation ranges have shown promising results under ideal lighting. For instance, Vipin (2012) achieved a 99% detection rate using handcrafted rules in RGB and YCbCr, and Binti Zaidi et al. (2015) reported 100% accuracy with YCbCr on still images. Celik and Ma (2008) and Marbach et al. (2006) both found that separating luminance from chrominance can help reduce the impact of variable lighting. More recently, Giwa and Benkrid (2024) proposed a novel flame-optimized color space using machine learning principles (clustering and meta heuristics), achieving a 20% F1-score improvement and highlighting the potential of tailoring color representations for fire detection.

Despite their simplicity and speed, color-based methods are highly susceptible to false positives, especially from fire-colored objects or reflections (Jain et al., 2020). Several works have attempted to mitigate this by incorporating additional visual cues. For example, Chen et al. (2004), Celik et al. (2007); Celik and Demirel (2009), Marbach et al. (2006) and Borges and Izquierdo (2010) designed systems that incorporated motion, flicker patterns, or area consistency checks, which perform well on video. Additionally, methods like measuring the 10Hz oscillation frequency of flames (Ko et al., 2009) or applying Gaussian Mixture Model subtraction to track candidate fire regions (Khalil et al., 2021) are used to detect fire pixels. However, these temporal techniques are not applicable to still images. This limitation motivates the integration of texture features, which provide spatial descriptors useful for distinguishing fire from non-fire objects with similar color properties.

Texture analysis has been explored as a complement to color information. Gabor filters (Gabor, 1946), known for their ability to capture local frequency and orientation, are particularly effective at highlighting the chaotic, multiscale texture of flames. Chino et al. (2015) introduced a system called BoWFire, which combined pixel-wise color and texture analysis to detect fire in still images, significantly reducing false alarms. Similarly, Borges and Izquierdo (2010) proposed a model that fused six features—including boundary roughness, red channel skewness, and surface coarseness—and processed them through a Bayesian classifier to distinguish fire regions, achieving a low false positive rate of 0.68%. Gomes et al. (2014) applied a combination of computer vision techniques; color-based segmentation, background subtraction, frequency analysis, and wavelet-based texture modeling to detect fires in real-world scenarios, achieving a 93.1% detection rate.

In parallel, preprocessing steps such as dehazing and contrast enhancement have been shown to improve segmentation performance in noisy conditions. Techniques like the Dark Channel Prior (He et al., 2009), CLAHE (Pizer et al., 1987), and Retinex-based color restoration (Guo et al., 2010) are often applied to restore visual quality before fire detection. Another approach involves polarization filtering, which mitigates atmospheric scatter-

ing by blocking light based on its polarization direction. Schechner et al. (2003) developed a dehazing method that leverages the fact that airlight—light scattered by atmospheric particles—is partially polarized, whereas light reflected directly from objects is mostly unpolarized. By comparing images captured through a polarizer at different orientations, this method estimates the contribution of airlight and isolates the haze components. However, its practical use is limited by the need for multiple images captured with a polarizing lens. Peng et al. (2020) extended this by introducing an airlight correction module and local light filtering in HSV space to handle artificial lighting distortions. Although these enhancements are effective, they still require robust feature extraction downstream to maintain high accuracy across diverse environments.

Taken together, these studies support a growing consensus that hybrid systems—particularly those combining color segmentation with texture analysis—offer a promising path forward for static-image fire detection. Our work builds on this insight by comparing the effectiveness of Gabor texture filtering when combined with four different color spaces (L*a*b, HSV, YCbCr, RGB), with the goal of identifying the most reliable feature combination for robust pixel-level fire classification.

3 Methodology

Our proposed fire detection pipeline consists of five stages: preprocessing, feature extraction, feature selection, classifier training, and post-processing. We begin by applying resizing and edge-preserving smoothing to prepare the input images. Next, we extract both spectral and texture features, aiming to capture the distinct visual characteristics of fire. These features are then analyzed and selected based on their discriminative power before being used to train a supervised classifier. Finally, morphological operations are applied to refine the segmentation masks, improving spatial consistency and reducing noise. Each stage is described in detail in the following sections.

3.1 Preprocessing

Preprocessing is a crucial step in our pipeline, particularly because our feature extraction stage relies on capturing subtle texture and color patterns that can be easily disrupted by noise or image compression artifacts. Rather than applying a standard smoothing filter such as Gaussian blur which often degrades edge information, we opt for a bilateral filter. Bilateral filter is a non-linear technique that smooths images while preserving edge sharpness.

The bilateral filter operates by combining both spatial proximity and intensity similarity when weighting neighboring pixels (Aswatha et al., 2011). This is particularly beneficial for fire segmentation, as fire regions often exhibit high-frequency details i.e flame contours, texture edges that should not be lost during denoising. Moreover, fire is typically characterized by strong local gradients in both brightness and color, and edge-preserving filters help maintain the integrity of these gradients for downstream feature extraction.

Formally, for a given pixel p, the filtered value $I'(p)$ is calculated as:

$$I'(p) = \frac{1}{W_p} \sum_{q \in \Omega} G_\sigma(\|p - q\|) \cdot G_\rho(\|I(p) - I(q)\|) \cdot I(q)$$

where G_σ is a spatial Gaussian weighting function, G_ρ is a range (intensity) Gaussian, W_p is a normalizing factor and Ω is the local neighborhood of pixel p.

This preprocessing step is applied to all images in the dataset before feature extraction. We also make sure that images feeding to the next stage are of consist size.

3.2 Feature Extraction

The accuracy of pixel-wise fire detection largely depends on the quality and relevance of the extracted features. In this stage, we compute two complementary types of features: spectral and textural. This hybrid approach leverages the distinctive visual characteristics of fire.

3.2.1 Spectral Feature Extraction

To characterize the color properties of fire pixels, we extract features from multiple color spaces: RGB, HSV, YCbCr, and CIELAB (L*a*b), resulting in a 12-dimensional feature space. These spaces were chosen for their widespread use in fire detection literature. Each color space offers a different representation of chromatic and luminance information, which can help in capturing the unique visual signatures of fire across varying

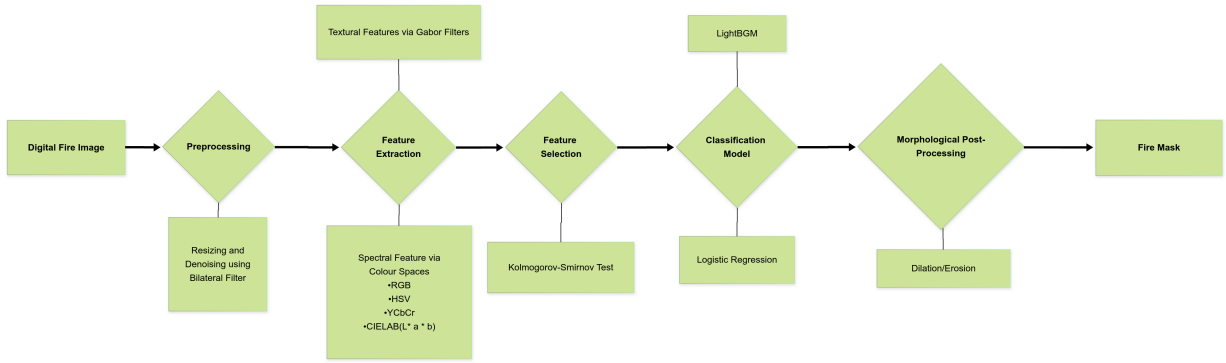

Figure 1: Overview of the proposed fire detection pipeline. The process involves extracting color features from multiple color spaces, computing Gabor texture features, selecting a subset of the most informative features, and training classifiers on the resulting compact feature set. The output is a binary mask.

lighting conditions and backgrounds. In RGB, fire pixels typically show high red intensity; in HSV, they cluster around specific hue and saturation values; in YCbCr, flames often exhibit strong responses in the Cr channel; and in L*a*b, fire tends to have high lightness and distinct a/b chromatic values. Combining them provides a more complete view of fire pixel spectral characteristics. However, this high-dimensional space also introduces redundancy as many of the channels are correlated, and not all contribute equally to distinguishing fire from non-fire pixels.

3.2.2 Textural Feature via Gabor Filters

Color alone is not always sufficient for reliable segmentation, particularly in low-contrast or noisy conditions where color differences between fire and background are subtle. To address this, we incorporate Gabor filtering to capture spatial texture cues of fire, such as chaotic, high-frequency patterns and directional structures. Gabor filters are biologically inspired, mimicking the response of the human visual cortex to textures, and are well-suited for detecting localized frequency and orientation information in an image.

The 2D Gabor filter is defined as:

$$g(x, y; \lambda, \theta, \psi, \sigma, \gamma) = e^{\left(-\frac{x'^2+\gamma^2 y'^2}{2\sigma^2}\right)} \cos\left(2\pi\frac{x'}{\lambda} + \psi\right)$$

where:

$$x' = x\cos\theta + y\sin\theta, \quad y' = -x\sin\theta + y\cos\theta$$

Here, λ is the wavelength of the sinusoidal factor, θ is the orientation of the normal to the parallel stripes, ψ is the phase offset, σ is the standard deviation of the Gaussian envelope, and γ controls the aspect ratio. By convolving each image with a bank of Gabor filters at multiple orientations and scales, we obtain a high-dimensional texture descriptor for each pixel.

3.3 Feature Selection

After extracting a high-dimensional set of features, including 12 spectral channels from multiple color spaces and a 16 Gabor texture responses, the next step is to identify and retain the most discriminative subset. This step is critical to improve model generalization, reduce computational overhead, and prevent overfitting, particularly when training on limited data.

We evaluate each individual feature using the Kolmogorov–Smirnov (KS) test (Massey Jr, 1951), which quantifies the pixel-level distributional difference between fire and non-fire pixel values. The KS statistic quantifies the maximum difference between the empirical cumulative distribution functions of the two classes, offering a non-parametric measure of distributional divergence. We chose the KS test due to its sensitivity to both location and shape differences in distributions and its minimal assumptions about the underlying data. Features with high KS (≥ 0.5) statistics indicate stronger separation between fire and non-fire pixels. The results are given in the next section.

3.4 Classification Model

To perform binary pixel-wise classification, we train two types of supervised models: *logistic regression* and

LightGBM (Ke et al., 2017), a gradient boosting decision tree classifier. Logistic regression serves as a simple linear baseline that models the log-odds of fire presence using a weighted combination of features. It is well-suited for linearly separable patterns, offering interpretability and low risk of overfitting.

In contrast, LightGBM captures nonlinear interactions between color and texture cues. It can learn complex decision boundaries and is better equipped to handle variations in lighting, texture, and background clutter. By comparing both models, we evaluate the trade-offs between simplicity and flexibility in our feature space.

3.5 Morphological Post-processing

After classification, the predicted binary masks often contain small isolated errors—such as scattered false positives or fragmented fire regions—due to pixel-level noise and local ambiguities. To address this, we apply morphological operations as a post-processing step to refine the output and improve spatial coherence.

Specifically, we use binary morphological operations such as opening (erosion followed by dilation) to remove small noise patches, and closing (dilation followed by erosion) to fill small holes within detected fire regions. These operations preserve the general shape of the segmented areas while improving visual consistency. The result is a cleaner, more interpretable binary fire mask that aligns better with human perception of fire boundaries.

4 Results

4.1 Spectral Features Analysis

To assess the discriminating power of raw color information for fire detection, we performed the Kolmogorov–Smirnov test on each individual color channel across four color spaces. The table (1) below summarizes the KS test results. The results highlight the top 5 color channels for detecting fire pixels.

The Kolmogorov–Smirnov test results reveal significant distributional differences between fire and non-fire pixels across most color channels. The Cb channel exhibits the highest KS statistic (0.7), indicating strong discriminative power, followed by the R, Cr, and V channels (all with KS statistics above 0.57). These results suggest that chrominance (Cb, Cr) and intensity-based channels (R, V) are particularly effective in separating fire from non-fire pixels. On the other hand, the a and B channels show minimal separation, with the B channel's KS statistic close to zero. This indicates that these features provide little to no discrimination for fire detection in this dataset.

While individual color channels such Cb, R, V, and Cr show strong discriminative power, using these top-performing channels may introduce redundancy. Many of the color spaces are nonlinear transformations of one another and capture overlapping information. Including all channels can increase model complexity, introduce noise, and lead to overfitting. To mitigate these issues, we applied Principal Component Analysis to the selected color feature set. PCA reduces dimensionality by projecting the data onto a new set of orthogonal axes (principal components) that capture the directions of maximum variance. This transformation helps to decorrelate the original features, compress the data efficiently, and enhance interpretability.

Our analysis revealed that the first two principal components explain over 95% of the total variance in the selected 5 colors, as shown in Figure 2. This indicates that most of the information contained in the 5 most informative color channels can be retained with just two uncorrelated components. The loadings reveal that PC1 contrasts red chrominance (Cr) against blue/yellow components (Cb and b), effectively separating fire-colored pixels from cooler backgrounds. PC2 is dominated by R and V, capturing overall intensity and brightness—characteristics strongly associated with fire. Pc3 involves strong negative contributions from both Cr and Cb, suggesting a chrominance suppression direction useful for distinguishing saturated fire from ambiguous

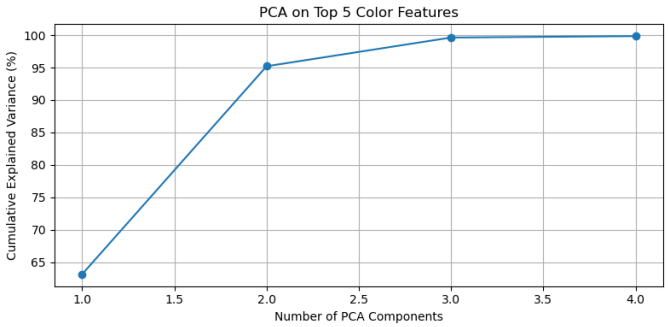

Figure 2: Cumulative explained variance of principal components derived from top 5 color features.

Table 1: KS Test Results for Color Channels

Channel	Non-Fire Mean	Non-Fire Std	Fire Mean	Fire Std	Abs Mean Diff	KS Statistic
Cb	116.8	20.2	75.5	26.2	41.3	0.7
R	102.8	74.9	215.6	48.8	112.8	0.6
Cr	140.5	20.4	171.0	21.9	30.5	0.6
V	106.8	76.1	215.7	48.8	108.9	0.6
b	114.4	21.4	84.2	21.7	30.2	0.6
S	108.5	81.7	184.3	65.6	75.8	0.4
Y	85.3	66.3	155.3	57.9	70.0	0.4
L	84.5	69.0	147.3	60.6	62.8	0.4
G	80.2	67.4	142.6	69.4	62.4	0.4
H	44.4	51.8	16.1	11.0	28.3	0.3
a	131.7	11.8	132.5	21.4	0.9	0.3
B	65.5	66.4	62.2	64.2	3.3	0.0

regions. PC4 contrasts V and R, potentially identifying bright, low-red areas such as the inner core of a flame.

Table 2: PCA Loadings for Color Features (First 4 Principal Components)

Channel	PC1	PC2	PC3	PC4
R	-0.1	0.8	0.0	-0.6
V	0.3	0.6	-0.1	0.6
b	0.6	-0.1	0.2	-0.5
Cr	-0.5	0.0	-0.6	-0.1
Cb	0.5	-0.1	-0.7	-0.2

4.2 Gabor Features evaluation

We generated a bank of Gabor kernels using multiple configurations of orientation, wavelength, and aspect ratio. The parameter choices are detailed as follows:

- **Orientation** (θ): We used four orientations: 0, $\frac{\pi}{4}$, $\frac{\pi}{2}$, and $\frac{3\pi}{4}$, which cover the primary axes and diagonal directions to capture edges at multiple angles.
- **Wavelength** (λ): We set the wavelength of the sinusoidal factor to $\{4, 8\}$, which controls the frequency of the texture being detected. Lower values are sensitive to finer textures, while higher values respond to coarser patterns.
- **Aspect Ratio** (γ): We tested both circular ($\gamma = 1.0$) and elliptical ($\gamma = 0.5$) shapes of the Gaussian envelope to allow for detection of both isotropic and elongated features.
- **Phase Offset** (ψ): Fixed to 0, ensuring symmetric filter responses.
- **Kernel Size** (ksize) and **Standard Deviation** (σ): We tested 3 different kernel size (3,7,11) with normal standard devation.

This configuration resulted in a total of $4 \times 2 \times 2 = 16$ distinct Gabor filters for each kernel size, each capturing unique texture characteristics. These kernels were then convolved with the input images to generate a 16-dimensional Gabor feature vector for each pixel.

KS test results for Gabor filter with kernel size of 7 is shown in table 3. Across all filters, we observe consistently large differences in mean values between the two classes, with absolute mean differences exceeding 100 in most cases and reaching as high as 612.9 for *gabor14*. These substantial differences suggest that fire and non-fire pixels elicit notably different responses from the Gabor filters. Furthermore, the KS statistic for all features is approximately 0.43, indicating a moderate but reliable distributional shift between the fire and non-fire responses for every Gabor kernel. Notably, some filters, such as *gabor14, gabor6,gabor 2*, and *gabor10*, exhibit both large absolute mean differences and strong KS statistics, highlighting their ability to capture unique spatial signatures associated with fire. These filters have higher frequency responses and elliptical shape that match common fire contours Refer to table 4 to learn about each gabor feature.

Despite the consistent discriminative power across filters, the similarity in KS statistics and overlapping mean structures (e.g., among *gabor15, gabor3, gabor7*) suggest a high degree of correlation or redundancy among

Table 3: Descriptive Statistics and KS Test for Gabor Features

Feature	Non-Fire Mean	Non-Fire Std	Fire Mean	Fire Std	Abs Mean Diff	KS Statistic
gabor_14	768.2	587.8	1381.1	508.7	612.9	0.43
gabor_6	768.2	587.8	1381.0	509.0	612.8	0.43
gabor_2	726.8	558.3	1312.6	485.5	585.8	0.43
gabor_10	727.1	558.8	1307.4	482.9	580.4	0.43
gabor_3	393.4	304.9	714.2	265.9	320.8	0.43
gabor_15	393.5	305.0	713.9	265.6	320.4	0.43
gabor_7	393.5	305.0	713.9	265.6	320.4	0.43
gabor_11	393.4	305.0	713.3	265.3	319.9	0.43
gabor_12	321.4	248.2	580.6	216.7	259.2	0.43
gabor_4	321.4	248.2	580.5	217.0	259.1	0.43
gabor_0	287.4	226.1	525.1	201.2	237.7	0.43
gabor_8	287.7	226.7	520.6	196.4	232.9	0.43
gabor_1	155.6	123.9	286.0	111.2	130.5	0.43
gabor_13	155.8	123.4	285.4	109.3	129.6	0.43
gabor_5	155.8	123.4	285.4	109.4	129.5	0.43
gabor_9	155.7	124.2	284.3	108.7	128.6	0.43

the Gabor features. We choose top 4 gabor response to include in the textural feature set. This results are lower for kernel size of 3 and consistent for kernel size 11. We avoid using PCA on the gabor features to maintain the spatial context.

4.3 Model Evaluation

The experiments in our paper use the diverse dataset originally presented by Chino et al. Chino et al. (2015). This dataset consists of 226 images of various resolutions captured under diverse real-world conditions, specifically curated to challenge the robustness of fire detection models. For the evaluation and training of our fire detection model, we separated this data into training and testing sets using a stratified 80/20 random split.

The dataset has two distinct classes, 119 images containing 'fire' in numerous emergency situations varying from building and car fires, to wildfires, to riots. The other 107 images containing negative examples, built to pose an extreme challenge for fire detection models as they contain images with similar color distributions to fire such as sunsets, and red/yellow colored objects. For evaluating our models, the dataset includes 119 ground-truth pixel-level masks which were manually extracted by human experts. Since fire pixels are significantly outnumbered by non-fire pixels in real-world imagery, the original dataset was highly imbalanced (1:21 ratio). Figure 3 shows the statistics of our dataset. To reduce model bias and ensure fair training, we constructed a balanced dataset using a 1:1 ratio of fire to non-fire pixels by undersampling non fire pixels.

Both models were tuned using cross-validation and grid search. The logistic regression model was tuned by selecting the regularization strength C based on validation performance, with the best value found at $C = 10$. For LightGBM, hyperparameter tuning identified the optimal configuration as *num_leaves = 63* and *max_depth = -1*, enabling the model to fully grow trees without depth restriction. We evaluate the performance of logistic regression and lightGBM on different color spaces and our selected feature set, which consists of the top 5 color channels and the top 4 Gabor responses from the KS test. We aim to compare our proposed features with the different color spaces and reported evaluation metrics such as accuracy, precision, recall, and F1-score, in addition to false positive rate (FPR), in our tables.

$$\text{Accuracy} = \frac{TP + TN}{TP + FP + TN + FN}$$

$$\text{Precision} = \frac{TP}{TP + FP}$$

$$\text{Recall} = \frac{TP}{TP + FN}$$

$$\text{F1-score} = 2 \cdot \frac{\text{Precision} \cdot \text{Recall}}{\text{Precision} + \text{Recall}}$$

The performance of logistic regression across different feature sets is summarized in Table 5. Among the individual color spaces tested, RGB, HSV, LAB, and

Table 4: Interpretation of Gabor Feature Indices

Gabor Index	Orientation (θ)	Wavelength (λ)	Aspect Ratio (γ)	Shape	Description
gabor_0	0	4	0.5	Elliptical	Horizontal, fine texture
gabor_1	0	4	1.0	Circular	Horizontal, fine texture
gabor_2	0	8	0.5	Elliptical	Horizontal, coarse texture
gabor_3	0	8	1.0	Circular	Horizontal, coarse texture
gabor_4	$\frac{\pi}{4}$	4	0.5	Elliptical	Diagonal (45°), fine texture
gabor_5	$\frac{\pi}{4}$	4	1.0	Circular	Diagonal (45°), fine texture
gabor_6	$\frac{\pi}{4}$	8	0.5	Elliptical	Diagonal (45°), coarse texture
gabor_7	$\frac{\pi}{4}$	8	1.0	Circular	Diagonal (45°), coarse texture
gabor_8	$\frac{\pi}{2}$	4	0.5	Elliptical	Vertical, fine texture
gabor_9	$\frac{\pi}{2}$	4	1.0	Circular	Vertical, fine texture
gabor_10	$\frac{\pi}{2}$	8	0.5	Elliptical	Vertical, coarse texture
gabor_11	$\frac{\pi}{2}$	8	1.0	Circular	Vertical, coarse texture
gabor_12	$\frac{3\pi}{4}$	4	0.5	Elliptical	Diagonal (135°), fine texture
gabor_13	$\frac{3\pi}{4}$	4	1.0	Circular	Diagonal (135°), fine texture
gabor_14	$\frac{3\pi}{4}$	8	0.5	Elliptical	Diagonal (135°), coarse texture
gabor_15	$\frac{3\pi}{4}$	8	1.0	Circular	Diagonal (135°), coarse texture

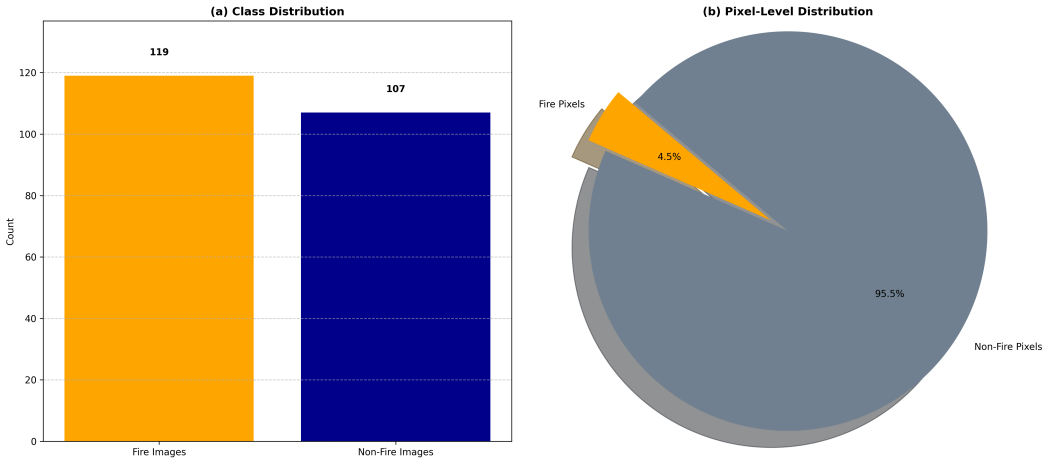

Figure 3: Information about our dataset, used for training the classifiers (before balancing).

YCrCb—model performance remains relatively close, with accuracies ranging from 84.74% to 86.33% and F1 scores around 86. The HSV feature set achieves the highest recall (89.96%) but also incurs the highest false positive rate (17.30%), indicating a trade-off between sensitivity and specificity. In contrast, the model trained on our selected feature set, which combines five color channels with four Gabor responses, outperforms all baseline feature sets across every metric. It achieves the highest accuracy (89.04%), precision (87.75%), recall (90.75%), and F1 score (89.22%), while also reducing the false positive rate to 12.67%. This strong performance reflects an improved balance between detecting true fire pixels and minimizing false alarms.

Table 6 presents the performance of the LightGBM classifier across different feature sets. All color space-based models achieve high recall and F1 scores close to 90, demonstrating the capacity of LightGBM to leverage even raw spectral features effectively. However, these models still exhibit relatively higher false positive rates. In comparison, our engineered feature set delivers the strongest overall performance. It achieves the highest accuracy (90.68%), precision (87.26%), recall (95.27%), and F1 score (91.09%), while also lowering the false positive rate to 13.92%. This reflects not only a higher sensitivity to fire pixels but also better control over false alarms compared to single color space models.

We also tried using principle component of the selected

Table 5: Logistic Regression Performance Across Feature Sets

Feature Set	Accuracy	Precision	Recall	F1 Score	FPR
RGB	86.15	85.07	87.70	86.36	15.39
HSV	86.33	83.87	89.96	86.81	17.30
LAB	84.74	84.34	85.33	84.83	15.84
YCrCb	86.14	85.07	87.66	86.34	15.39
Our Selected Features	**89.04**	**87.75**	**90.75**	**89.22**	**12.67**

Table 6: LightGBM Performance Across Feature Sets

Feature Set	Accuracy	Precision	Recall	F1 Score	FPR
RGB	89.19	85.27	94.75	89.76	16.36
HSV	89.42	85.44	95.03	89.98	16.20
LAB	88.94	84.69	95.06	89.57	17.18
YCrCb	89.18	85.00	95.16	89.79	16.79
Our Selected Features	**90.68**	**87.26**	**95.27**	**91.09**	**13.92**

color to reduce the dimensions of the features, but it led to lower performance. This suggests that, although PCA reduced redundancy among color channels, it may have also removed subtle but important discriminative information, leading to slightly lower performance compared to using the original color features.

These results reinforce the benefit of adding Gabor-based texture information to spectral information. LightGBM's ability to model non-linear relationships allows it to fully exploit the richness of our handcrafted feature set, resulting in improved generalization and robustness in fire detection. Figure 4 presents the results of applying our trained model to three out-of-distribution (OOD) images. Under noisy conditions such as the presence of smoke, our model performed relatively well, successfully identifying fire regions despite visual ambiguity.

5 Conclusion and Future Work

This study presented a pixel-wise fire detection pipeline using color and texture features. While individual color spaces showed limitations, combining multiple color channels—each capturing different spectral characteristics of fire with Gabor texture filters significantly improved performance, particularly by reducing the false positive rate, which is critical in detection systems. Through statistical analysis, we showed that most discriminating color channels for detecting fire pixels from background are *Cr, Cb, V, b*. Our method outperformed all baseline models across key metrics, achieving up to 90.68% accuracy with LightGBM and 89.04% with logistic regression. These results highlight the value of integrating complementary spectral and spatial information, even in relatively simple classification models.

Although effective, the current pipeline can be further improved. Future work includes exploring learned features via convolutional neural networks (CNNs), particularly once deep learning methods are allowed; extending the approach to video sequences by incorporating temporal and motion-based features; and investigating more diverse Gabor configurations or alternative texture descriptors to improve generalization. Finally, training on real-world datasets with greater variability and noise would help validate the system's robustness and deployment readiness.

Code Availability

The code used in this study is publicly available on GitHub[1].

[1] https://github.com/jacobtizel/fire-finder

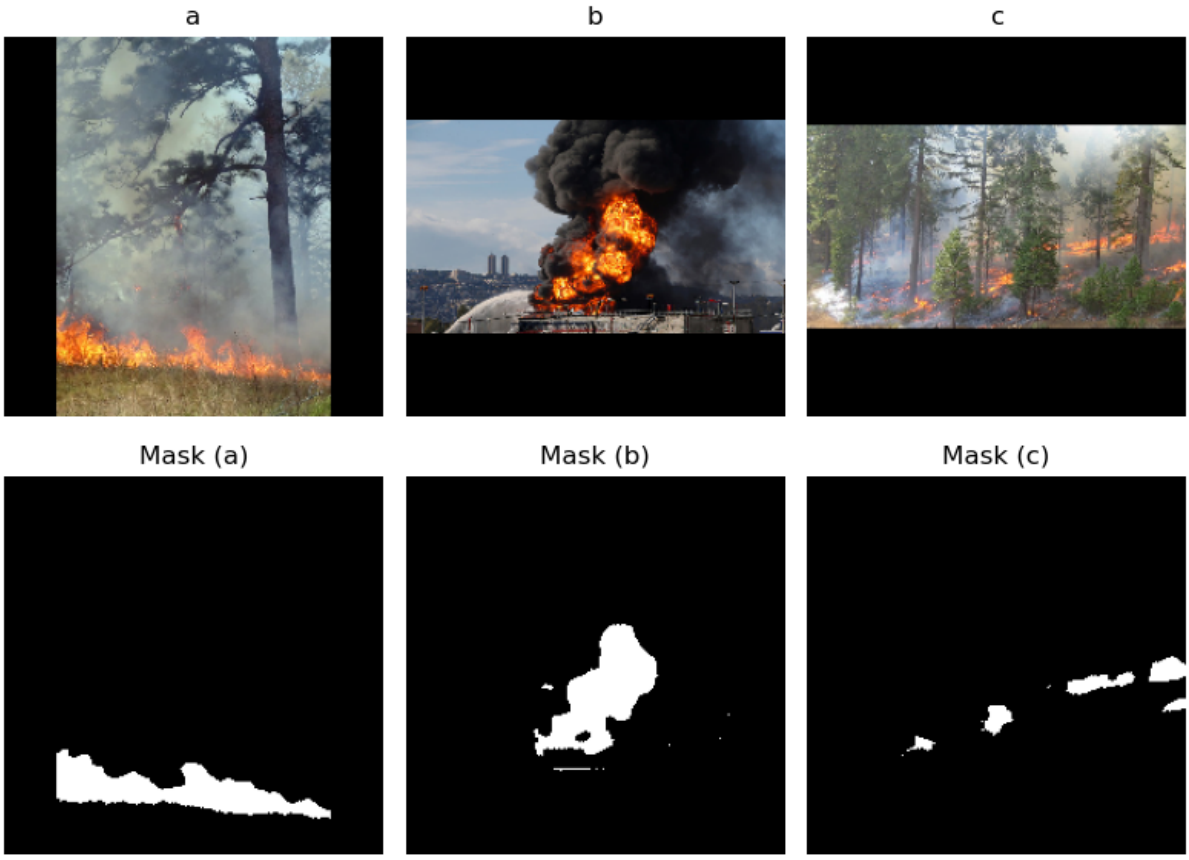

Figure 4: Three out-of-distribution images and their corresponding masks generated by our pipeline.

References

Ajay Bhosle, Abhinandan Ambekar, S. B. V. I. (2024). Flame recognition: Image processing solutions for rapid fire detection. *International Journal of Innovative Research in Technology*, 11(1):35–40.

Aswatha, S. M., Mukhopadhyay, J., and Bhowmick, P. (2011). Image denoising by scaled bilateral filtering. In *2011 Third National Conference on Computer Vision, Pattern Recognition, Image Processing and Graphics*, pages 122–125.

Binti Zaidi, N. I., binti Lokman, N. A. A., bin Daud, M. R., Achmad, H., and Chia, K. A. (2015). Fire recognition using rgb and ycbcr color space. *ARPN Journal of Engineering and Applied Sciences*, 10(21):9786–9790.

Borges, P. V. K. and Izquierdo, E. (2010). A probabilistic approach for vision-based fire detection in videos. *IEEE transactions on circuits and systems for video technology*, 20(5):721–731.

Celik, T. and Demirel, H. (2009). Fire detection in video sequences using a generic color model. *Fire safety journal*, 44(2):147–158.

Celik, T., Demirel, H., Ozkaramanli, H., and Uyguroglu, M. (2007). Fire detection using statistical color model in video sequences. *Journal of Visual Communication and Image Representation*, 18(2):176–185.

Celik, T. and Ma, K.-K. (2008). Computer vision based fire detection in color images. In *2008 IEEE Conference on Soft Computing in Industrial Applications*, pages 258–263. IEEE.

Chen, T.-H., Wu, P.-H., and Chiou, Y.-C. (2004). An early fire-detection method based on image processing. In *2004 International Conference on Image Processing, 2004. ICIP'04.*, volume 3, pages 1707–1710. IEEE.

Chino, D. Y., Avalhais, L. P., Rodrigues, J. F., and Traina, A. J. (2015). Bowfire: detection of fire in still

images by integrating pixel color and texture analysis. In *2015 28th SIBGRAPI conference on graphics, patterns and images*, pages 95–102. IEEE.

Gabor, D. (1946). Theory of communication. part 1: the analysis of information. j inst electr eng-part iii: Radio commun eng 93 (26): 429–441.

Ghali, R., Jmal, M., Souidene Mseddi, W., and Attia, R. (2020). Recent advances in fire detection and monitoring systems: A review. In *Proceedings of the 8th International Conference on Sciences of Electronics, Technologies of Information and Telecommunications (SETIT'18), Vol. 1*, pages 332–340. Springer.

Giwa, O. and Benkrid, A. (2024). A new flame-based colour space for efficient fire detection. *IET Image Processing*, 18(5):1229–1244.

Gomes, P., Santana, P., and Barata, J. (2014). A vision-based approach to fire detection. *International Journal of Advanced Robotic Systems*, 11(9):149.

Guo, F., Cai, Z., Xie, B., and Tang, J. (2010). Automatic image haze removal based on luminance component. In *2010 6th International conference on wireless communications networking and mobile computing (WiCOM)*, pages 1–4. IEEE.

He, K., Sun, J., and Tang, X. (2009). Single image haze removal using dark channel prior. In *2009 IEEE Conference on Computer Vision and Pattern Recognition*, pages 1956–1963.

Jain, P., Coogan, S. C., Subramanian, S. G., Crowley, M., Taylor, S., and Flannigan, M. D. (2020). A review of machine learning applications in wildfire science and management. *Environmental Reviews*, 28(4):478–505.

Ke, G., Meng, Q., Finley, T., Wang, T., Chen, W., Ma, W., Ye, Q., and Liu, T.-Y. (2017). Lightgbm: A highly efficient gradient boosting decision tree. In *Proceedings of the 31st International Conference on Neural Information Processing Systems (NeurIPS)*, pages 3146–3154. Curran Associates Inc.

Khalil, A., Rahman, S. U., Alam, F., Ahmad, I., and Khalil, I. (2021). Fire detection using multi color space and background modeling. *Fire technology*, 57:1221–1239.

Ko, B. C., Cheong, K.-H., and Nam, J.-Y. (2009). Fire detection based on vision sensor and support vector machines. *Fire Safety Journal*, 44(3):322–329.

Marbach, G., Loepfe, M., and Brupbacher, T. (2006). An image processing technique for fire detection in video images. *Fire safety journal*, 41(4):285–289.

Massey Jr, F. J. (1951). The kolmogorov-smirnov test for goodness of fit. *Journal of the American Statistical Association*, 46(253):68–78.

Peng, Y.-T., Lu, Z., Cheng, F.-C., Zheng, Y., and Huang, S.-C. (2020). Image haze removal using airlight white correction, local light filter, and aerial perspective prior. *IEEE Transactions on Circuits and Systems for Video Technology*, 30(5):1385–1395.

Pizer, S. M., Amburn, E. P., Austin, J. D., Cromartie, R., Geselowitz, A., Greer, T., ter Haar Romeny, B., Zimmerman, J. B., and Zuiderveld, K. (1987). Adaptive histogram equalization and its variations. *Computer vision, graphics, and image processing*, 39(3):355–368.

Schechner, Y. Y., Narasimhan, S. G., and Nayar, S. K. (2003). Polarization-based vision through haze. *Applied optics*, 42(3):511–525.

Toulouse, T., Rossi, L., Campana, A., Celik, T., and Akhloufi, M. A. (2017). Computer vision for wildfire research: An evolving image dataset for processing and analysis. *Fire Safety Journal*, 92:188–194.

Umamaheshwaran, R., Bijker, W., and Stein, A. (2006). Image mining for modeling of forest fires from meteosat images. *IEEE Transactions on Geoscience and Remote Sensing*, 45(1):246–253.

Vipin, V. (2012). Image processing based forest fire detection. *International Journal of Emerging Technology and Advanced Engineering*, 2(2):87–95.

Xiong, W. (2020). Research on fire detection and image information processing system based on image processing. In *2020 International Conference on Advance in Ambient Computing and Intelligence (ICAACI)*, pages 106–109. IEEE.

Zarkasi, A., Nurmaini, S., Stiawan, D., Amanda, C. D., et al. (2019). Implementation of fire image processing for land fire detection using color filtering method. In *Journal of Physics: Conference Series*, volume 1196, page 012003. IOP Publishing.